ACS Chemical Neuroscience

Letter

pubs.acs.org/chemneuro

Opening of the Blood-Brain Barrier Tight Junction Due to Shock Wave Induced Bubble Collapse: A Molecular Dynamics Simulation Study

Ardeshir Goliaei,[†,∥] Upendra Adhikari,[‡,∥] and Max L. Berkowitz*[,‡]

[†]Department of Biochemistry and Biophysics and Program in Molecular and Cellular Biophysics, and [‡]Department of Chemistry, University of North Carolina at Chapel Hill, Chapel Hill, North Carolina 27599, United States

ABSTRACT: Passage of a shock wave across living organisms may produce bubbles in the blood vessels and capillaries. It was suggested that collapse of these bubbles imposed by an impinging shock wave can be responsible for the damage or even destruction of the blood-brain barrier. To check this possibility, we performed molecular dynamics computer simulations on systems that contained a model of tight junction from the blood-brain barrier. In our model, we represent the tight junction by two pairs of interacting proteins, claudin-15. Some of the simulations were done in the absence of a nanobubble, some in its presence. Our simulations show that when no bubble is present in the system, no damage to tight junction is observed when the shock wave propagates across it. In the presence of a nanobubble, even when the impulse of the shock wave is relatively low, the implosion of the bubble causes serious damage to our model tight junction.

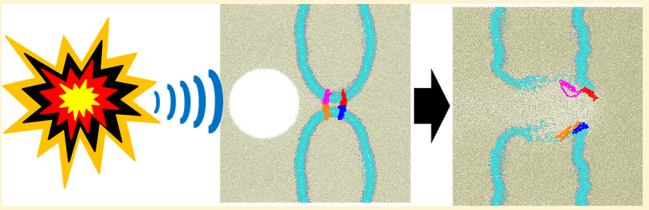

KEYWORDS: *Blood-brain barrier, shock wave, cavitation effect, traumatic brain injury, claudin protein, tight junction*

Lately, it was shown that the cavitation effect plays a very important role in the ultrasound assisted drug delivery to specific areas of the human body, including brain areas.[1−7] Delivering drugs to the brain is problematic due to the presence of the blood-brain barrier (BBB), a system that controls the exchange of chemicals between blood and brain regions. Therefore, implosions of microbubbles loaded with drugs, implosions that occur due to cavitation effect induced by the traveling ultrasound, weaken or destroy the BBB, opening the way for drug permeation into the brain. Recently, it was suggested that pressure waves created by blasts, that produce injury in the brain, so-called blast-induced traumatic brain injury (bTBI), may be also connected to damaged BBB.[8−15] Among different reasons that may cause damage to BBB, the cavitation effect (that is present due to implosion of bubbles, microscopic or nanoscopic in size, and created in blood during the passage of shock waves from the blast), was also considered as a possible reason. While some experimental work[8−14] and very recent computational work that used continuum modeling[15] investigated the connection between bTBI (or TBI in general) and damage to the BBB, no work has yet appeared gearing toward understanding the molecular picture behind this connection.

Computer simulations proved to be a very efficient tool in providing detailed and often molecular detailed pictures of events occurring in biological processes.[16−19] Detailed simulations describing motion of every atom are used when detailed information is required, for example, to understand such process as a change in the secondary structure of a protein. When the length and time scales of the processes are large in comparison with atomic scales, one can use coarse grained (CG) simulations where, for example, a group of atoms is represented by an effective particle and the interaction between atoms is reduced to interaction between these kinds of effective particles, as it is done in the force field called MARTINI.[20] Initially constructed to describe model lipid membranes, MARTINI was extended to describe interactions between membranes and proteins,[21] often producing a successful nanoscopic description of the processes taking place in these systems.[22] We used MARTINI to study interactions of antimicrobial peptides, such as melittin and/or magainin, with lipid membranes.[23−25] Very recently, we also used MARTINI to study shock wave induced implosions of bubbles situated next to lipid bilayers and the damage to bilayers due to such implosions.[26−28]

In this paper, we report the results from our computational study on how the shock wave induced bubble implosions (cavitation effect) influence the strength of the BBB. Since no previous molecular or even coarse-grained models of BBB are available in the literature, we propose here a first such model. The BBB, as are most of the biological machineries, is quite complicated, especially on a detailed molecular or nanoscopic level. To simulate the BBB damage due to cavitation, our first model needs to be simplified and we concentrated our study on the tight junction (TJ) region between the endothelial cells. In our model, the TJ connecting the gap between two adjacent cell membranes is represented by two pairs of typical TJ proteins, claudins, specifically claudins-15. We chose claudin-15 because its crystal structure was available[29] and, more importantly, it is homologically related to claudin-5,[30] which is abundant in brain

Published: June 15, 2015

DOI: 10.1021/acschemneuro.5b00116
ACS Chem. Neurosci. 2015, 6, 1296−1301

capillaries.[31] We monitored the degree of the connection between claudin-15 protein pairs when they were exposed to the cavitation effect and observed that bubble implosion plays a crucial role in the serious damage to our model BBB, indicating that the cavitation effect also suspected to exist in the human body after blasts may produce damage and even destroy the BBB, and thus be responsible for the brain damage produced in many blasts, even when they are mild.

RESULTS AND DISCUSSION

We described the interactions between molecules in our systems by using a coarse grained MARTINI force field with improved parameters for proteins[32] and polarizable water.[33] The improved parameters provide a more realistic description of the proteins and their interactions with lipid bilayers.[22,32] Since no structure is available for the interacting pair of claudin-15 situated in the extracellular region, we performed long molecular dynamics simulations to get such a structure (see Methods for details). To construct our model of TJ between two cells, we created a large oval shaped vesicle containing DPPC lipids solvated in water (9835 CG DPPC lipid molecules and 727 946 CG polarizable water molecules). On one of the sides of the vesicle, we placed two pairs of interacting claudin-15 proteins. Because of the periodic boundary conditions we use in our simulations, we actually simulate a stack of "cells" (our vesicles) connected through model TJ consisting of two pairs of interacting claudin-15 proteins. Figure 1 depicts the

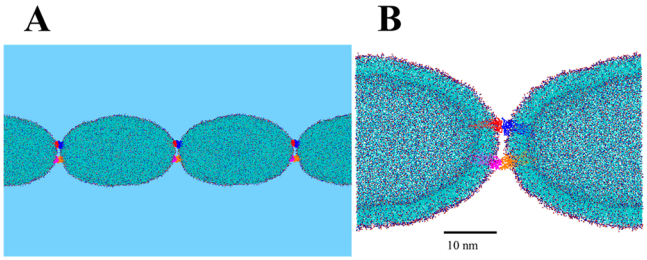

Figure 1. Initial configuration of the model TJ. (A) Simulation box (with no bubble present) periodically repeated in the $-X$ and $+X$ directions. Blue background represents water. (B) TJ part in the simulation box where more emphasis on the two pairs of proteins is highlighted. Each one of the interacting claudin-15 molecules is color coded to show the interacting partner.

stack (panel (A)) containing periodic images of our "cells" and the TJ between them; this picture is reminiscent of a picture of a stack of cells connected by TJ that surround a blood capillary. Panel (B) of Figure 1 shows the simulation unit cell containing parts of the membrane with the TJ between them. Following up on the initial preparation step, we expanded the size of the unit cell of our system in the Y and Z directions by adding CG MARTINI polarizable water. The expansion of number of water molecules to include 3 481 386 CG particles produced a box with sizes $54.0 \times 54.0 \times 144.4$ nm^3. This was done with the purpose to incorporate a bubble 30 nm in diameter in the water region located bellow the vesicle. The bubble (nanobubble) was created by removing all water molecules situated in a sphere of diameter 30 nm located in the vicinity of the TJ. The final large-sized unit cell (in some cases containing a bubble, in some without a bubble, to be able to study the effect of a bubble collapse on the integrity of the TJ by comparing results from simulations with and without the bubble collapse) was again equilibrated for another 10 ns, and after this equilibration period our production runs with shock waves impinging on the system were performed. Shock waves were generated by using the momentum mirror approach which was successfully applied in previous simulation work where shock waves were created.[26−28,34−36] The procedure we adopted to create shock waves is analogous to having a piston in our system that is moving toward the $+Z$ direction with velocity ν_p and reflecting all the particles coming into contact with it. We stopped the piston after a short time (τ_s), and allowed the created shock wave to move in the $+Z$ direction. By doing this, we produced a shock wave impulse traveling toward the TJ. In the present simulations, ν_p was 1.5 km/s and we performed simulations with two τ_s values: 2 and 5 ps. The shock wave velocity ν_s was calculated in systems containing pure CG polarizable water by measuring the speed of discontinuity in water density profile along the $+Z$ direction. The damage produced by the shock wave on the subject it hits is determined by the shock wave impulse (when no bubbles are present) that is given by the equation $I = \int_0^{t+} P(t)\, dt$, where $P(t)$ is the shock wave pressure on the membrane and t^+ is the duration of time it takes for the positive phase of the shock wave to pass.[37] Using the above formula, we calculated the impulse for systems with no bubbles. The shock wave velocities and impulses for cases when ν_p = 1.5 km/s and τ_s = 2 and 5 ps are presented in Table 1. This table

Table 1. Impulse and Velocity of the Shock Wave at the Time When It Hits the Bilayer for Different Piston Stopping Time (τ_s)

τ_s (ps)	impulse (I), mPa·s	shock velocity (ν_s), km/s
2	8.44	2.27
5	35.59	3.11

serves as a dictionary that translates values for parameters we use in simulations to parameters describing the shock wave speed and intensity, parameters that are used to report experimental measurements. As we can see from Table 1, the shock wave impulse in our simulations corresponds to impulses created by a very mild blast ($I \sim 8.5$ mPa·s when τ_s = 2 ps) and a mild blast ($I \sim 35.6$ mPa·s when τ_s = 5 ps).

The main results from our simulations can be seen depicted in Figures 2−5. In the absence of a nanobubble, the passage of a shock wave has a small effect on the interacting pairs of proteins, as can be seen in Figure 2. As the figure shows, following the shock passage, the interacting proteins in systems with no bubbles retain their contacts with one another and do not separate from each other. However, in the case of τ_s = 5 ps, upon the collapse of 30 nm in diameter nanobubble caused by the passage of the shock wave, a large change in properties of both vesicle and proteins in our system can be observed in Figure 2A. The vesicle parts next to proteins are expanded following the bombardment by high velocity water particles and their shape changes. The proteins completely lose their contacts and pairs become separate entities. On the other hand the effect is less pronounced when τ_s = 2 ps, as shown in Figure 2B. Although the proteins in the pair that were hit first (bottom pair in the figure) get separated, the degree of their separation is smaller compared to that in the case with τ_s = 5 ps; the proteins that were hit later (top pair in the figure) still keep their contact. In addition, the vesicle itself has not been changed substantially, as this happened in the case when τ_s = 5 ps. The secondary structure of the proteins also changed as a result of the bubble collapse, as again can be inferred from

DOI: 10.1021/acschemneuro.5b00116
ACS Chem. Neurosci. 2015, 6, 1296−1301

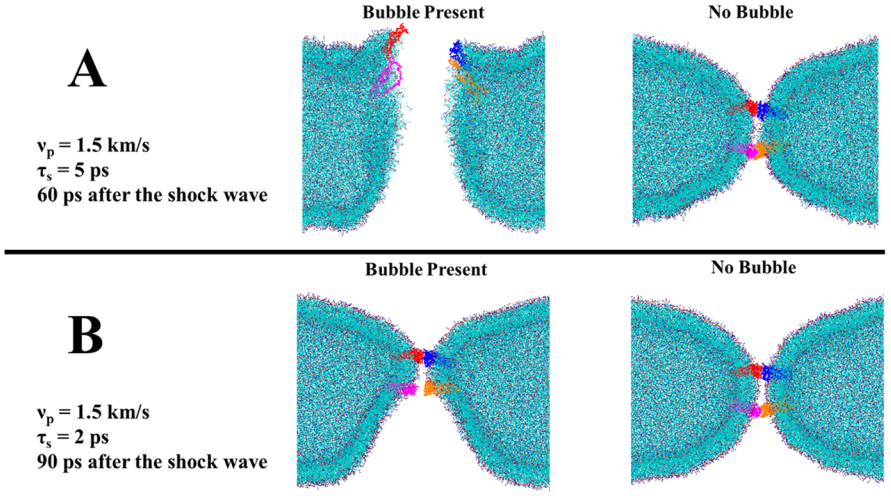

Figure 2. Shock wave simulations with and without a nanobubble. The figure shows the configuration of the vesicle and protein pairs after shock. Snapshot from the simulation (A) when τ_s = 5 ps and (B) when τ_s = 2 ps. In each panel, the resulting configuration when no bubble is present is on the right, whereas the case when the bubble is present is on the left.

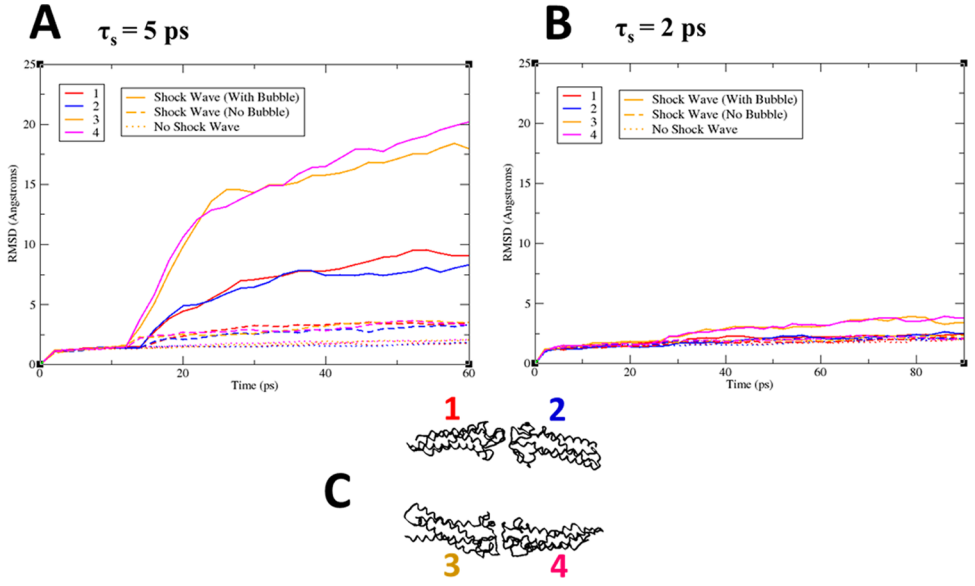

Figure 3. RMSD curves for each of the claudin-15 proteins. (A) Change of RMSD values over 60 ps shock wave simulation, when τ_s = 5 ps. (B) Change of RMSD over 90 ps of simulation when τ_s = 2 ps. Each graph is colored and corresponds to the numbered proteins shown in (C). RMSD values for simulation with the presence of bubble are represented by solid lines. Lines for results from shock wave simulation without bubbles are shown as dashed lines. As a control, simulations with no shock waves were also performed and the RMSD values were measured. They are presented in the graphs as dotted lines.

Figure 2. To quantify the change in the secondary structure of our proteins, values for the RMSD from the initial crystal structure were calculated and compared to the values obtained from simulations with no bubbles being present. Figure 3 shows the result of RMSD calculations for simulations performed in this study. Figure 3A shows a significant change in RMSD values for the two proteins on the bottom (3 and 4) and a smaller change for the two proteins on the top (1 and 2) when τ_s = 5 ps. Figure 3B shows that in the case when τ_s = 2 ps, the values for the RMSD were not that large. The fact that proteins 3 and 4 display large RMSD is expected, since these proteins are closer to the bubble when it collapses and hence they feel a greater force. In comparison, when there is no bubble present, RMSD values do not change significantly in time, as shown by dashed lines in both panels (A) and (B).

To analyze further the effect of bubble collapse on the proteins, the number of contacts between interacting partner proteins was measured. Figure 4A indicates that, as expected, when τ_s = 5 ps, the number of contacts between two interacting proteins drops to zero (complete separation) in the presence of the bubble. However, without a bubble present, no significant change in the number of contacts is seen during the 60 ps of shock wave simulation. On the other hand, when the τ_s = 2 ps, as Figure 4B shows, only the closest pair to the bubble loses contact completely (black curve), while the top pair (red curve) is still in contact, even after 90 ps of the simulation. An illustration of the structural dynamics of our model of TJ collapse, observed in simulations when the nanobubble was present (and when τ_s = 5 ps), is shown in Figure 5. As the simulation progresses, the bubble collapse causes a complete segregation of the two protein pairs and also causes the change

DOI: 10.1021/acschemneuro.5b00116
ACS Chem. Neurosci. 2015, 6, 1296−1301

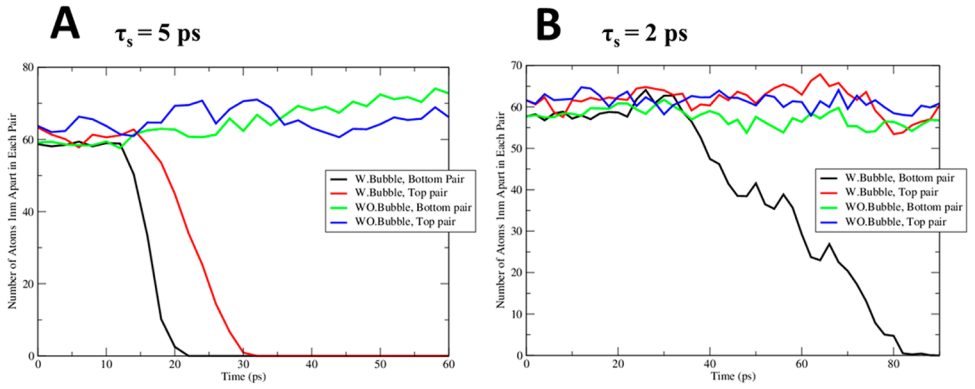

Figure 4. Number of contacts between interacting protein pairs. (A) Change in the number of contacts between interacting pairs during 60 ps of shock wave simulation when τ_s = 5 ps. (B) Change in contact number during 90 ps of simulation when τ_s = 2 ps. Black and red curves represent cases when a bubble is present, while green and blue lines represent cases when there is no bubble.

in the shape of the lipid vesicle, that gets elongated in the direction of the shock wave propagation.

CONCLUSION

Our computer simulations reported here were performed to study the effect of nanobubble collapse that, as it is suggested, can occur in blood capillaries after passage of the blast induced shock waves. It was also suggested that this collapse may cause damage to, or even destruction of, the BBB by damaging (destroying) the TJ between the BBB cells.[2,15] In our simulations we considered model systems with the TJ containing two pairs of the TJ protein, claudin-15. When no bubble was present in the system, we did not observe any damage done to the TJ upon passage of the shock wave. In cases when bubbles of 30 nm in diameter were present in the system, their collapse under the influence of a very mild shock wave with an impulse of ∼8 mPa·s produced some small amount of damage to the TJ. When the impulse of the shock wave was more than 4 times larger (but still remained mild in relative values, if compared with the impulse of 54 Pa·s observed in experiment when no damage to cell was done[37]), our model TJ was destroyed. Although our simulations were performed on relatively simple systems, they show the crucial role played by the presence of nanobubbles and the cavitation effect in causing severe damage to cell membranes and also proteins embedded in the cell membranes.

METHODS

Our molecular dynamics simulations were performed using Gromacs 4.6.6 package.[38−41] The initial structure of the protein in our study was the available crystal structure of claudin-15[29] (PDB ID: 4P79). To coarse grain the protein, the martinize.py script,[32] downloaded from the MARTINI force field website, was used. Cysteine residues 47 and 57 were linked together to emulate disulfide bonds in the extracellular region number one (ECL1). The claudin-15 protein carries a net negative charge of −1, and therefore, we also placed sodium ions (Na^+) into the system in numbers that were needed to neutralize the system.

The structure of the interacting pair of claudin-15 situated in the extracellular (ECL) region was obtained by performing long molecular dynamics simulations. Initially, one protein was inserted in a cylindrical pore created in the center of a DPPC (1,2-dipalmitoyl-*sn*-glycero-3-phosphocholine) bilayer containing a patch of 150 lipids. This bilayer together with the embedded protein was then replicated, rotated, and translated to the top of the first system so that the two ECL regions of each protein were in water facing each other, but not in contact with each other. This new system (a double bilayer with one protein in each bilayer) was then energy minimized, and a 1 μs molecular dynamics run was performed. During this run, the two proteins found each other and made a head-to-head contact after ∼100 ns. This contact was stable throughout the rest of the simulation, so we used the created claudin-15 pair as a model of our interacting proteins in the TJ. The 1 μs simulation was done using the NPT ensemble, with temperature kept at 320 K and pressure at 1.0 bar (semi-isotropic coupling) using the Berendsen coupling scheme.[42] The time constants for temperature and pressure coupling were 1 and 2 ps, respectively. Compressibility value for the pressure coupling was set to 3×10^{-4} bar^{-1}. The Lennard−Jones interaction cutoff value of 1.2 nm was used, and the "shift" scheme with a cutoff of 1.2 nm was applied for the electrostatics. The dielectric constant was set to 2.5, and the time step for the integration was 20 fs. The final box size was X = 7.25, Y = 7.25, and Z = 17.9 nm.

Since the goal of our simulations is to study how the proteins of TJ region respond to cavitation during the blast, it is important to have the correct density in our system. Therefore, prior to performing shock wave simulations, we continued the preparation of the system without the bubbles and equilibrated it for 100 ns using the NVT ensemble. To create the shock wave, we used the mirror approach when all the particles in the system move with certain velocity ν_p toward the mirror placed at the end of the box in the $-Z$ direction. The particles get reflected upon impact with the mirror, thus creating a shock wave with velocity ν_s larger than ν_p and moving in the $+Z$ direction. A 2 nm vacuum layer was added at the end of the $-Z$ direction to avoid the immediate contact between the particles and the mirror at the beginning of the simulation. All shock simulations were performed in the constant energy ensemble with the periodic boundary condition (PBC) turned off in the Z-direction. The time step of 4 fs was used. The cutoff value for the nonbonded interactions was 1.4 nm instead of the usual 1.2 nm, and the neighbors list was updated every 5 steps, instead of the usual 10. Each simulation with τ_s = 2 ps was performed for 90 ps and with τ_s = 5 ps for 60 ps, to make sure the shock front moved across the simulation box and exited on the end opposite from where it initiated. Since shock wave simulations were short in their duration, we performed a number of them, with different initial velocities, but corresponding to the same temperature. All the results were very similar for simulations done with the same value of τ_s. We presented here the results from one typical simulation in each case.

The pressure calculation was done using Gromacs-4.0.2_local pressure[43] version of Gromacs following the method developed by Ollila et al.[43] The dimension of the small cubes when discretizing the system was set to 0.5 nm.

To study the integrity of the protein pair in its contact, we analyzed the number of contact points between the pair using the Plumed 2.1 plug-in.[44] More specifically, we calculated how many atoms from the first protein are found at a certain distance (1 nm in our case) from the second protein of the same pair. The calculated value was considered

DOI: 10.1021/acschemneuro.5b00116
ACS Chem. Neurosci. 2015, 6, 1296−1301

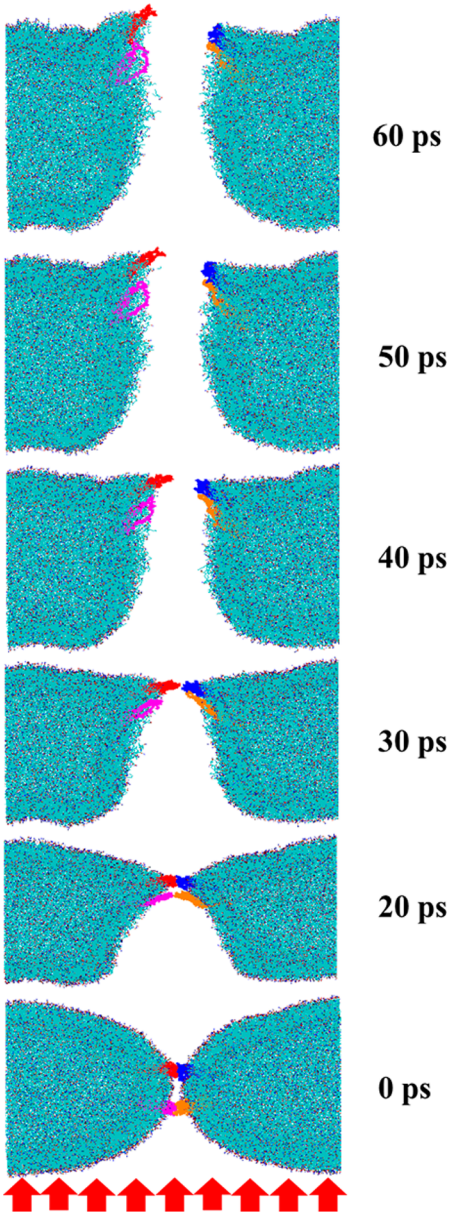

Figure 5. Overall progress of the simulation during the 60 ps shock wave propagation in a system when a 30 nm bubble is present and when τ_s = 5 ps. The frames are in the direction of increasing time when observed from the bottom-up. Red arrows at the bottom indicate the direction of the shock wave propagation.

as the number of contacts between the two interacting proteins in our study.

AUTHOR INFORMATION

Corresponding Author

*E-mail: maxb@unc.edu.

Author Contributions

‖A.G. and U.A. contributed equally to this work. A.G. and U.A. participated in the design of the simulations, performed the simulations and participated in the writing of the manuscript. M.L.B. directed the research, participated in the design of the simulations and writing of the manuscript.

Funding

The support by Grant N00014-14-1-0241 from the Office of Naval Research is gratefully acknowledged.

Notes

The authors declare no competing financial interest.

REFERENCES

(1) Zhao, Y.-Z., Du, L.-N., Lu, C.-T., Jin, Y.-G., and Ge, S.-P. (2013) Potential and problems in ultrasound-responsive drug delivery systems. *Int. J. Nanomed. 8*, 1621−1633.

(2) Liu, H.-L., Fan, C.-H., Ting, C.-Y., and Yeh, C.-K. (2014) Combining microbubbles and ultrasound for drug delivery to brain tumors: current progress and overview. *Theranostics 4*, 432−444.

(3) Husseini, G. A., Pitt, W. G., and Martins, A. M. (2014) Ultrasonically triggered drug delivery: Breaking the barrier. *Colloids Surf., B 123*, 364−386.

(4) Sheikov, N., McDannold, N., Vykhodtseva, N., Jolesz, F., and Hynynen, K. (2004) Cellular mechanisms of the blood-brain barrier opening induced by ultrasound in presence of microbubbles. *Ultrasound Med. Biol. 30*, 979−989.

(5) Vykhodtseva, N., McDannold, N., and Hynynen, K. (2008) Progress and problems in the application of focused ultrasound for blood-brain barrier disruption. *Ultrasonics 48*, 279−296.

(6) Liu, H.-L., Hua, M.-Y., Chen, P.-Y., Chu, P.-C., Pan, C.-H., Yang, H.-W., Huang, C.-Y., Wang, J.-J., Yen, T.-C., and Wei, K.-C. (2010) Blood-brain barrier disruption with focused ultrasound enhances delivery of chemotherapeutic drugs for glioblastoma treatment. *Radiology 255*, 415−425.

(7) McDannold, N., Arvanitis, C. D., Vykhodtseva, N., and Livingstone, M. S. (2012) Temporary disruption of the blood-brain barrier by use of ultrasound and microbubbles: Safety and efficacy evaluation in rhesus macaques. *Cancer Res. 72*, 3652−3663.

(8) Shlosberg, D., Benifla, M., Kaufer, D., and Friedman, A. (2010) Blood-brain barrier breakdown as a therapeutic target in traumatic brain injury. *Nat. Rev. Neurol. 6*, 393−403.

(9) Shetty, A. K., Mishra, V., Kodali, M., and Hattiangady, B. (2014) Blood brain barrier dysfunction and delayed neurological deficits in mild traumatic brain injury induced by blast shock waves. *Front. Cell. Neurosci. 8*, 232.

(10) Hue, C. D., Cao, S., Haider, S. F., Vo, K. V., Effgen, G. B., Vogel, E., Panzer, M. B., Bass, C. R. D., Meaney, D. F., and Morrison, B. (2013) Blood-brain barrier dysfunction after primary blast injury in vitro. *J. Neurotrauma 30*, 1652−1663.

(11) Abdul-Muneer, P. M., Schuetz, H., Wang, F., Skotak, M., Jones, J., Gorantla, S., Zimmerman, M. C., Chandra, N., and Haorah, J. (2013) Induction of oxidative and nitrosative damage leads to cerebrovascular inflammation in an animal model of mild traumatic brain injury induced by primary blast. *Free Radical Biol. Med. 60*, 282−291.

(12) Yeoh, S., Bell, E. D., and Monson, K. L. (2013) Distribution of blood-brain barrier disruption in primary blast injury. *Ann. Biomed. Eng. 41*, 2206−2214.

(13) Cho, H. J., Sajja, V. S. S. S., VandeVord, P. J., and Lee, Y. W. (2013) Blast induces oxidative stress, inflammation, neuronal loss and subsequent short-term memory impairment in rats. *Neuroscience 253*, 9−20.

(14) Tompkins, P., Tesiram, Y., Lerner, M., Gonzalez, L. P., Lightfoot, S., Rabb, C. H., and Brackett, D. J. (2013) Brain injury: neuro-inflammation, cognitive deficit, and magnetic resonance imaging in a model of blast induced traumatic brain injury. *J. Neurotrauma 30*, 1888−1897.

(15) Del Razo, M. J., Morofuji, Y., Meabon, J. S., Huber, B. R., Peskind, E. R., Banks, W. A., Mourad, P. D., Leveque, R. J., and Cook, D. G. (2015) Computational and in vitro studies of blast-induced blood-brain barrier disruption. arXiv:1503.09157.

(16) Warshel, A. (2002) Molecular Dynamics Simulations of Biological Reactions. *Acc. Chem. Res. 35*, 385−395.

(17) Karplus, M., and Kuriyan, J. (2005) Molecular dynamics and protein function. *Proc. Natl. Acad. Sci. U. S. A. 102*, 6679−6685.

(18) Adcock, S. A., and McCammon, J. A. (2006) Molecular dynamics: Survey of methods for simulating the activity of proteins. *Chem. Rev. 106*, 1589−1615.

DOI: 10.1021/acschemneuro.5b00116
ACS Chem. Neurosci. 2015, 6, 1296−1301

(19) Dodson, G. G., Lane, D. P., and Verma, C. S. (2008) Molecular simulations of protein dynamics: new windows on mechanisms in biology. *EMBO Rep. 9*, 144−150.
(20) Marrink, S. J., Risselada, H. J., Yefimov, S., Tieleman, D. P., and de Vries, A. H. (2007) The MARTINI force field: Coarse grained model for biomolecular simulations. *J. Phys. Chem. B 111*, 7812−7824.
(21) Monticelli, L., Kandasamy, S. K., Periole, X., Larson, R. G., Tieleman, D. P., and Marrink, S.-J. (2008) The MARTINI Coarse-Grained Force Field: Extension to Proteins. *J. Chem. Theory Comput. 4*, 819−834.
(22) Marrink, S. J., and Tieleman, D. P. (2013) Perspective on the Martini model. *Chem. Soc. Rev. 42*, 6801−6822.
(23) Santo, K. P., and Berkowitz, M. L. (2012) Difference between magainin-2 and melittin assemblies in phosphatidylcholine bilayers: results from coarse-grained simulations. *J. Phys. Chem. B 116*, 3021−3030.
(24) Santo, K. P., Irudayam, S. J., and Berkowitz, M. L. (2013) Melittin creates transient pores in a lipid bilayer: Results from computer simulations. *J. Phys. Chem. B 117*, 5031−5042.
(25) Goliaei, A., Santo, K. P., and Berkowitz, M. L. (2014) Local Pressure Changes in Lipid Bilayers Due to Adsorption of Melittin and Magainin-h2 Antimicrobial Peptides: Results from Computer Simulations. *J. Phys. Chem. B 118*, 12673−12679.
(26) Santo, K. P., and Berkowitz, M. L. (2014) Shock wave interaction with a phospholipid membrane: coarse-grained computer simulations. *J. Chem. Phys. 140*, 054906.
(27) Santo, K. P., and Berkowitz, M. L. (2014) Shock Wave Induced Collapse of Arrays of Nanobubbles Located Next to a Lipid Membrane: Coarse-Grained Computer Simulations. *J. Phys. Chem. B*, DOI: 10.1021/jp505720d.
(28) Adhikari, U., Goliaei, A., and Berkowitz, M. L. (2015) Mechanism of Membrane Poration by Shock Wave Induced Nanobubble Collapse: A Molecular Dynamics Study. *J. Phys. Chem. B 119*, 6225−6234.
(29) Suzuki, H., Nishizawa, T., Tani, K., Yamazaki, Y., Tamura, A., Ishitani, R., Dohmae, N., Tsukita, S., Nureki, O., and Fujiyoshi, Y. (2014) Crystal structure of a claudin provides insight into the architecture of tight junctions. *Science 344*, 304−307.
(30) Krause, G., Winkler, L., Mueller, S. L., Haseloff, R. F., Piontek, J., and Blasig, I. E. (2008) Structure and function of claudins. *Biochim. Biophys. Acta 1778*, 631−645.
(31) Haseloff, R. F., Dithmer, S., Winkler, L., Wolburg, H., and Blasig, I. E. (2015) Transmembrane proteins of the tight junctions at the blood−brain barrier: Structural and functional aspects. *Semin. Cell Dev. Biol. 38*, 16−25.
(32) De Jong, D. H., Singh, G., Bennett, W. F. D., Arnarez, C., Wassenaar, T. A., Schäfer, L. V., Periole, X., Tieleman, D. P., and Marrink, S. J. (2013) Improved Parameters for the Martini Coarse-Grained Protein Force Field. *J. Chem. Theory Comput. 9*, 687−697.
(33) Yesylevskyy, S. O., Schäfer, L. V, Sengupta, D., Marrink, S. J., and Levitt, M. (2010) Polarizable water model for the coarse-grained MARTINI force field. *PLoS Comput. Biol. 6*, e1000810 DOI: 10.1371/journal.pcbi.1000810.
(34) Vedadi, M., Choubey, A., Nomura, K., Kalia, R. K., Nakano, A., Vashishta, P., and van Duin, A. C. T. (2010) Structure and Dynamics of Shock-Induced Nanobubble Collapse in Water. *Phys. Rev. Lett. 105*, 014503.
(35) Nomura, K.-I., Kalia, R. K., Nakano, A., Vashishta, P., van Duin, A. C. T., and Goddard, W. A. (2007) Dynamic transition in the structure of an energetic crystal during chemical reactions at shock front prior to detonation. *Phys. Rev. Lett. 99*, 148303.
(36) Choubey, A., Vedadi, M., Nomura, K., Kalia, R. K., Nakano, A., and Vashishta, P. (2011) Poration of lipid bilayers by shock-induced nanobubble collapse. *Appl. Phys. Lett. 98*, 023701.
(37) Kodama, T., Hamblin, M. R., and Doukas, A. G. (2000) Cytoplasmic molecular delivery with shock waves: Importance of impulse. *Biophys. J. 79*, 1821−1832.
(38) Hess, B., Kutzner, C., van der Spoel, D., and Lindahl, E. (2008) GROMACS 4: Algorithms for Highly Efficient, Load-Balanced, and Scalable Molecular Simulation. *J. Chem. Theory Comput. 4*, 435−447.
(39) Van Der Spoel, D., Lindahl, E., Hess, B., Groenhof, G., Mark, A. E., and Berendsen, H. J. C. (2005) GROMACS: Fast, flexible, and free. *J. Comput. Chem. 26*, 1701−1718.
(40) Lindahl, E., Hess, B., and van der Spoel, D. (2001) GROMACS 3.0: A package for molecular simulation and trajectory analysis. *J. Mol. Model. 7*, 306−317.
(41) Berendsen, H. J. C., van der Spoel, D., and van Drunen, R. (1995) GROMACS: A message-passing parallel molecular dynamics implementation. *Comput. Phys. Commun. 91*, 43−56.
(42) Berendsen, H. J. C., Postma, J. P. M., van Gunsteren, W. F., DiNola, A., and Haak, J. R. (1984) Molecular dynamics with coupling to an external bath. *J. Chem. Phys. 81*, 3684.
(43) Ollila, O., Risselada, H., Louhivuori, M., Lindahl, E., Vattulainen, I., and Marrink, S. (2009) 3D Pressure Field in Lipid Membranes and Membrane-Protein Complexes. *Phys. Rev. Lett. 102*, 078101.
(44) Tribello, G. A., Bonomi, M., Branduardi, D., Camilloni, C., and Bussi, G. (2014) PLUMED 2: New feathers for an old bird. *Comput. Phys. Commun. 185*, 604−613.

DOI: 10.1021/acschemneuro.5b00116
ACS Chem. Neurosci. 2015, 6, 1296−1301